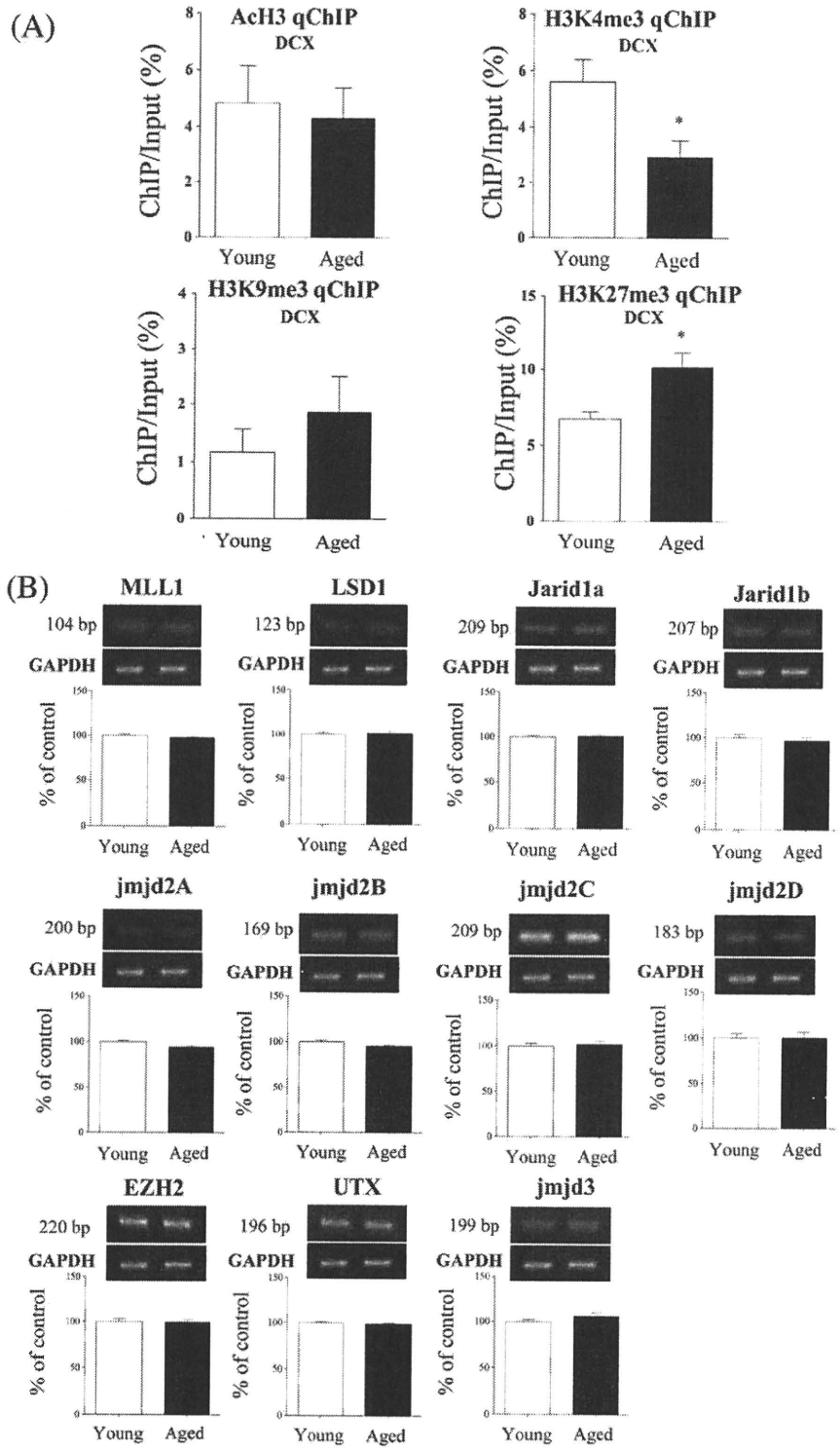

Fig. 2. **A**: Stable changes in histone modifications in the hippocampus in aged mice. ChIP assays were performed to measure the levels of several histone modifications at the doublecortin (DCX) promoter in the hippocampus using specific antibodies for each modification state. Levels of promoter enrichment were quantified by quantitative PCR. Histone H3 was not altered at DCX. Significant changes in acetylation (AcH3) or H3K9 trimethylation (H3K9me3) were not detected at the DCX promoter region. Histone H3K4 trimethylation (H3K4me3) was decreased at the DCX promoter region in aged mice. $^*P < 0.05$ vs. the young group. Histone H3K27 trimethylation (H3K27me3) was increased at the DCX promoter region in aged mice. $^*P < 0.05$ vs. the young group. **B**: Upper: Representative RT-PCR for MLL1 (a H3K4 methyltransferase), LSD1, Jarid1a and Jarid1b (H3K4 demethylases), jmjd2A, jmjd2B, jmjd2C and jmjd2D (H3K9 demethylases), and EZH2 (a H3K27 methyltransferase), and UTX and jmjd3 (H3K27 demethylases). mRNAs in the hippocampus obtained from young and aged mice. Lower: The intensity of the bands was semiquantified using NIH Image software. The value for mRNA was normalized by that for the internal standard glyceraldehyde-3-phosphate dehydrogenase (GAPDH) mRNA. The value for aged mice is expressed as a percentage of the increase in young mice. Each column represents the mean ± S.E.M. of six samples.

is associated with transcribed chromatin. In contrast, trimethylation of H3K9 and H3K27 generally correlates with repression (Bernstein et al., 2007). In agreement with the PCR assay, we found here that aging caused a significant decrease in H3K4 trimethylation and a significant increase in H3K27 trimethylation at the doublecortin gene. In contrast, we failed to find any changes in the H3K9 trimethylation and hyperacetylation of H3 at the doublecortin gene. These findings suggest that aging produces a dramatic decrease in the expression of the neuronal progenitor doublecortin along with epigenetic modifications in the hippocampus.

Histone methylation is dynamically regulated by a plethora of methylases and demethylases (Swigut and Wysocka, 2007). In the present study, aging failed to change the mRNA expression of several methylases and demethylases including MLL1 (a H3K4 methyltransferase), LSD1, Jarid1a and Jarid1b (H3K4 demethylases), jmjd2A, jmjd2B, jmjd2C and jmjd2D (H3K9 demethylases), EZH2 (a H3K27 methyltransferase), and UTX and jmjd3 (H3K27 demethylases). These findings suggest that aging causes a dramatic decrease in neurogenesis accompanied by epigenetic modification related to the decreased expression of doublecortin without changing the expression of their associated histone methylases and demethylases in the hippocampus.

In conclusion, although further investigation is still required, the present findings suggest that decreased expression of the migrated neural progenitor doublecortin associated with histone modification may be, at least in part, involved in an aging-dependent decrease in neurogenesis in the hippocampus. Since the methylation of H3K27 is especially considered to play a critical role in the long-lasting silencing of targeted gene expression (Swigut and Wysocka, 2007), the present finding of the epigenetically repressive modulation of neural progenitors could allow us to better understand the mechanism of aging-dependent hippocampal dysfunction.

REFERENCES

Barnes CA. 1994. Normal aging: Regionally specific changes in hippocampal synaptic transmission. Trends Neurosci 17:13–18.

Bernstein BE, Meissner A, Lander ES. 2007. The mammalian epigenome. Cell 128:669–681.

Bliss TV, Collingridge GL. 1993. A synaptic model of memory: Long-term potentiation in the hippocampus. Nature 361:31–39.

Eriksson PS, Perfilieva E, Bjork-Eriksson T, Alborn AM, Nordborg C, Peterson DA, Gage FH. 1998. Neurogenesis in the adult human hippocampus. Nat Med 4:1313–1317.

Geinisman Y, DeToledo-Morrell L, Morrell F, Persina IS, Rossi M. 1992. Age-related loss of axospinous synapses formed by two afferent systems in the rat dentate gyrus as revealed by the unbiased stereological dissector technique. Hippocampus 2:437–444.

Gravina S, Vijg J. 2009. Epigenetic factors in aging and longevity. Pflugers Arch (in press).

Hwang IK, Yoo KY, Yi SS, Kwon YG, Ahn YK, Seong JK, Lee IS, Yoon YS, Won MH. 2008. Age-related differentiation in newly generated DCX immunoreactive neurons in the subgranular zone of the gerbil dentate gyrus. Neurochem Res 33:867–872.

Jaenisch R, Bird A. 2003. Epigenetic regulation of gene expression: How the genome integrates intrinsic and environmental signals. Nat Genet 33 (Suppl):245–254.

Kempermann G, Kuhn HG, Gage FH. 1997. More hippocampal neurons in adult mice living in an enriched environment. Nature 386: 493–495.

Kuhn HG, Dickinson-Anson H, Gage FH. 1996. Neurogenesis in the dentate gyrus of the adult rat: Age-related decrease of neuronal progenitor proliferation. J Neurosci 16:2027–2033.

Lichtenwalner RJ, Forbes ME, Bennett SA, Lynch CD, Sonntag WE, Riddle DR. 2001. Intracerebroventricular infusion of insulin-like growth factor-I ameliorates the age-related decline in hippocampal neurogenesis. Neuroscience 107:603–613.

Lois C, Alvarez-Buylla A. 1993. Proliferating subventricular zone cells in the adult mammalian forebrain can differentiate into neurons and glia. Proc Natl Acad Sci USA 90:2074–2077.

Nakajima T, Yamashita S, Maekita T, Niwa T, Nakazawa K, Ushijima T. 2009. The presence of a methylation fingerprint of *Helicobacter pylori* infection in human gastric mucosae. Int J Cancer 124:905–910.

Swigut T, Wysocka J. 2007. H3K27 demethylases, at long last. Cell 131:29–32.

Takeshima H, Yamashita S, Shimazu T, Niwa T, Ushijima T. 2009. The presence of RNA polymerase II, active or stalled, predicts epigenetic fate of promoter CpG islands. Genome Res 19:1974–1982.

Tsankova NM, Kumar A, Nestler EJ. 2004. Histone modifications at gene promoter regions in rat hippocampus after acute and chronic electroconvulsive seizures. J Neurosci 24:5603–5610.

Tsankova N, Renthal W, Kumar A, Nestler EJ. 2007. Epigenetic regulation in psychiatric disorders. Nat Rev Neurosci 8:355–367.

van Praag H, Kempermann G, Gage FH. 1999. Running increases cell proliferation and neurogenesis in the adult mouse dentate gyrus. Nat Neurosci 2:266–270.

SYNAPSE 64:721–728 (2010)

Short Communication

Enhanced IL-1β Production in Response to the Activation of Hippocampal Glial Cells Impairs Neurogenesis in Aged Mice

NAOKO KUZUMAKI,[1] DAIGO IKEGAMI,[1] SATOSHI IMAI,[1] MICHIKO NARITA,[1] RIE TAMURA,[1] MARIE YAJIMA,[1] ATSUO SUZUKI,[1] KAZUHIKO MIYASHITA,[1] KEIICHI NIIKURA,[1] HIDEYUKI TAKESHIMA,[2] TAKAYUKI ANDO,[2] TOSHIKAZU USHIJIMA,[2] TSUTOMU SUZUKI,[1] AND MINORU NARITA[1]*

[1]*Department of Toxicology, Hoshi University School of Pharmacy and Pharmaceutical Sciences, 2-4-41 Ebara, Shinagawa-ku, Tokyo 142-8501, Japan*

[2]*Carcinogenesis Division, National Cancer Center Research Institute, 5-1-1 Tsukiji, Chuo-ku, Tokyo 104-0045, Japan*

[Correction to title made after initial online publication.]

KEY WORDS aging; hippocampus; astrocytes; microglia; IL-1β; neurogenesis

A variety of mechanisms that contribute to the accumulation of age-related damage and the resulting brain dysfunction have been identified. Recently, decreased neurogenesis in the hippocampus has been recognized as one of the mechanisms of age-related brain dysfunction. However, the molecular mechanism of decreased neurogenesis with aging is still unclear. In the present study, we investigated whether aging decreases neurogenesis accompanied by the activation of microglia and astrocytes, which increases the expression of IL-1β in the hippocampus, and whether in vitro treatment with IL-1β in neural stem cells directly impairs neurogenesis. Ionized calcium-binding adaptor molecule 1 (Iba1)-positive microglia and glial fibrillary acidic protein (GFAP)-positive astrocytes were increased in the dentate gyrus of the hippocampus of 28-month-old mice. Furthermore, the mRNA level of IL-1β was significantly increased without related histone modifications. Moreover, a significant increase in lysine 9 on histone H3 (H3K9) trimethylation at the promoter of NeuroD (a neural progenitor cell marker) was observed in the hippocampus of aged mice. In vitro treatment with IL-1β in neural stem cells prepared from whole brain of E14.5 mice significantly increased H3K9 trimethylation at the NeuroD promoter. These findings suggest that aging may decrease hippocampal neurogenesis via epigenetic modifications accompanied by the activation of microglia and astrocytes with the increased expression of IL-1β in the hippocampus. **Synapse 64:721–728, 2010.**

INTRODUCTION

The stability of life is constantly threatened by a wide range of internal and external stressors, and, under these circumstances, active maintenance is required to protect the integrity of the organism. It is widely accepted that aging is caused by the gradual, lifelong accumulation of a wide variety of molecular and cellular damage.

The hippocampus is one of the few areas of the rodent brain that continues to produce neurons postnatally (Eriksson et al., 1998). Neurogenesis in the dentate gyrus (DG) of the hippocampus occurs throughout the life of rodents. The aging hippocampus undergoes a variety of structural and functional alterations, which may be accompanied by decreased hippocampal neurogenesis (Kuhn et al., 1996).

Microglia are CNS-resident, macrophage-like cells of hematopoietic origin that play a role in the homeo-

This article was published online on 23 March 2010. An error was subsequently identified. This notice is included in the online and print versions to indicate that both have been corrected 24 May 2010.

*Correspondence to: Minoru Narita, Department of Toxicology, Hoshi University School of Pharmacy and Pharmaceutical Sciences, 2-4-41 Ebara, Shinagawa-ku, Tokyo, 142-8501, Japan. E-mail: narita@hoshi.ac.jp

Received 1 December 2009; Accepted 16 February 2010

DOI 10.1002/syn.20800

Published online 23 March 2010 in Wiley InterScience (www.interscience.wiley.com).

stasis of the healthy CNS and as immune surveillance cells in response to infection and injury. When neurons are injured as a result of aging or neurodegeneration, microglia become activated via the release of ATP, neurotransmitters, growth factors or cytokines, chemokines, ion changes in the local environment, or a loss of inhibitor molecules displayed by healthy neurons (Lucin and Wyss-Coray, 2009).

In there role as cells that provide multiple forms of support to the CNS, astrocytes are beginning to be appreciated as suppliers of critical survival and differentiation factors to neurons and other glial cells. Recent studies have suggested that astrocytes may express cytokines, chemokines, and growth factors as well as neurotransmitters throughout life, and not only in the developing fetus. Further studies on brain damage have suggested that, like microglia, astrocytes may be over-activated with aging (Labourdette and Eclancher, 2002).

Cytokines and chemokines are small, mostly secreted proteins that were originally characterized as immune modulators, but they have subsequently been found to mediate a diverse array of functions in glial cells that reside in the brain as well as peripheral glial cells and immunocells. Recently, it has been reported that excessive IL-1β contributes to the antineurogenic effect (Koo and Duman, 2008). Thus, in this study, we investigated whether aging increases IL-1β in the hippocampus associated with the activation of microglia and astrocytes, and whether in vitro treatment with IL-1β affects neural stem cell differentiation.

This study was conducted in accordance with the Guiding Principles for the Care and Use of Laboratory Animals, Hoshi University, as adopted by the Committee on Animal Research of Hoshi University, which is accredited by the Ministry of Education, Culture, Sports, Science and Technology of Japan. All efforts were made to minimize the number of animals used and their suffering.

Two- and from 24- to 28-month-old C57BL/6J mice (Jackson Laboratories, Bar Harbor, ME) were used in this study. Animals were kept in a room with an ambient temperature of 23 ± 1°C and a 12-h light/dark cycle (lights on 8:00 AM–8:00 PM). Food and water were available ad libitum. This study was approved by the Animal Research Committee of Hoshi University.

Mice were deeply anesthetized with isoflurane (3%) and perfusion-fixed with 4% paraformaldehyde (pH 7.4). The brain was then quickly removed and the hippocampus was rapidly dissected and postfixed in 4% paraformaldehyde for 2 h. The hippocampus was permeated with 20% sucrose for 1 day and 30% sucrose for 2 days, and then frozen in an embedding compound (Sakura Finetechnical, Tokyo, Japan). All samples were stored at −30°C until use. The sections were cut transversely at a thickness of 8 μm on a cryostat (Leica CM1510, Leica Microsystems, Heidelberg, Germany). The hippocampus sections were blocked in 10% normal goat serum in 0.01M phosphate-buffered saline (PBS) for 1 h at room temperature. Each primary antibody was diluted in 0.01M PBS containing 10% normal goat serum glial fibrillary acidic protein (GFAP), (1:20 Nichirei, Tokyo, Japan) or ionized calcium-binding adaptor molecule 1, (Iba1) (1:130 Wako Pure Chemicals, Osaka, Japan), and incubated for 2 days overnight at 4°C. The samples were then rinsed and incubated with the appropriate secondary antibody conjugated with Alexa 488 (Invitrogen, Carlsbad, CA) for 2 h at room temperature. The slides were then coverslipped with Perma-Fluor Aqueous mounting medium (Immunon, Pittsburgh, PA). Fluorescence of immunolabeling was detected using a light microscope (Olympus AX-70; Olympus, CO, Tokyo, Japan) and a Radiance 2000 laser-scanning microscope (BioRad, Richmond, CA), and photographed with a digital camera (Polaroid PDMCII/OL; Olympus, CO, Tokyo, Japan).

Two- and from 24- to 28-month-old mice (Jackson Laboratories, Bar Harbor, ME) were used for Western blotting. Each hippocampus was individually homogenized in ice-cold buffer A containing 20 mM Tris-HCl (pH 7.5), 2 mM EDTA, 0.5 mM EGTA, 1 mM phenylmethylsulfonyl fluoride, 25 μg of leupeptin per ml, 0.1 mg of aprotinin per mL, and 0.32M sucrose. The homogenate was centrifuged at 1000 × *g* for 10 min and the supernatant was ultracentrifuged at 100,000 × *g* for 30 min at 4°C. The pellets were washed with buffer B (buffer A without sucrose) and then ultracentrifuged at 100,000 × *g* for 30 min. The final pellets were retained as the membranous fraction for Western blotting at −80°C until the assay. Protein concentration in the samples was assayed by the method of Bradford et al. (Bradford, 1976). An aliquot of tissue sample was diluted with an equal volume of 2× electrophoresis sample buffer (Protein Gel Loading Dye-2×; Amresco, Solon, OH) containing 2% sodium dodecyl sulfate (SDS) and 10% glycerol with 0.2M dithiothreitol. Proteins (10–20 μg/lane) were separated by size on 4–20% SDS-polyacrylamide gradient gel using the buffer system, and then transferred to nitrocellulose membranes in Tris-glycine buffer containing 25 mM Tris and 192 mM glycine. For immunoblot detection, the membranes were blocked in Tris-buffered saline (TBS) containing 1% nonfat dried milk with 0.1% Tween 20 (Bio-Rad Laboratories, Hercules, CA) for 1 h at room temperature with agitation. The membrane was incubated with primary antibody diluted in TBS containing 1% nonfat milk with 0.1% Tween 20 [1:1000 GFAP (Nichirei, Tokyo, Japan), 1:1000 Iba1 (Wako Pure Chemicals, Osaka, Japan)] overnight at 4°C. The membrane was washed in TBS containing 0.05% Tween 20 (TTBS), and then incubated for 2 h at room temperature with

horseradish peroxidase-conjugated antirabbit IgG (Southern Biotechnology Associates, Birmingham, AL) diluted 1:10,000 in TBS containing 1% nonfat dried milk with 0.1% Tween 20. To control for validation in loading, we assayed the expression of a housekeeping gene by Western blot analysis. After incubation with primary and secondary antibodies, the membrane was then re-probed with mouse anti-GAPDH polyclonal antibody [GFAP: 1:200,000 in TBS containing 1% nonfat milk with 0.1% Tween 20, Iba1: 1:50,000 in 5% nonfat milk (Chemicon International, Temecula, CA)] for 1 h, and then incubated with anti-mouse secondary antibody conjugated with horseradish peroxidase (1:10,000) for 2 h at room temperature. The antigen–antibody peroxidase complex was finally detected by enhanced chemiluminescence (Pierce, Rockford, IL) according to the manufacturer's instructions and visualized by exposure to Amersham Hyperfilm (Amersham Life Sciences, Arlington Heights, IL).

Total RNA in the hippocampus of aged mice was extracted using the SV Total RNA Isolation system (Promega, Madison, WI) following the manufacturer's instructions. Purified total RNA was quantified spectrophotometrically at A_{260}. To prepare first-strand cDNA, 1 μg of RNA was incubated in 100 μl of buffer containing 10 mM dithiothreitol, 2.5 mM $MgCl_2$, dNTP mixture, 50 U of reverse transcriptase II (Invitrogen, Carlsbad, CA) and 0.1 mM oligo-$dT_{12\text{-}18}$ (Invitrogen, Carlsbad, CA). Each gene was amplified in 50 μl of PCR solution containing 0.8 mM $MgCl_2$, dNTP mixture, and DNA polymerase with synthesized primers: IL-1β, F; 5′-CAC TAG GTT TGC CGA GTA GAT CTC-3′, R; 5′-GTG CTG CCT AAT GTC CCC TTG AAT C-3′, NeuroD, F; 5′-GCA TGC ACG GGC TGA ACG C-3′, R; 5′-GGG ATG CAC CGG GAA GGA AG-3′, GAPDH, F; 5′-CCC ACG GCA AGT TCA ACG G-3′, R; 5′-CTT TCC AGA GGG GCC ATC CA-3′. Samples were heated to 94°C for 30 s, 55°C for 1 min, and 72°C for 1 min. The final incubation was at 72°C for 7 min. The mixture was run on 2% agarose gel electrophoresis with the indicated markers and primers for the internal standard glyceraldehyde-3-phosphate dehydrogenase. The agarose gel was stained with ethidium bromide and photographed with UV transillumination. The intensity of the bands was analyzed and semiquantified by computer-assisted densitometry using ImageJ software.

Fast SYBR Green Master Mix (Applied Biosystems, Foster City, CA) was used as the basis for the reaction mixture in the real-time PCR assay. Each gene prepared by the above procedure was amplified in 20 ml of a PCR solution containing 10 ml of the Fast SYBR Green Master Mix with synthesized primers: NeuroD, F; 5′-GCA TGC ACG GGC TGA ACG C-3′, R; 5′-GGG ATG CAC CGG GAA GGA AG-3′, β-actin, F; 5′-CAG CTT CTT TGC AGC TCC TT-3′, R; 5′-TCA CCC ACA TAG GAG TCC TT-3′. In addition to each sample, each test run included a no-target control that contained reaction mixture and PCR-grade water. PCR with a StepOnePlus™ (Applied Biosystems, CA) was performed with the following cycling conditions: 95°C for 20 s, followed by 45 cycles of 95°C for 3 s and 60°C for 30 s. Fluorescence detection was conducted after each extension step.

A ChIP assay was performed as described previously (Tsankova et al., 2004; Takeshima et al., 2009) with minor modifications. Briefly, mouse hippocampus tissue was dissected as described above and cross-linked, and the tissue was then lysed. Fifteen μg of soluble chromatin was incubated with 2 μg of specific antibodies; against acetylated histone H3 (Millipore, Billerica, MA); H3K4 trimethylation (Wako Pure Chemicals, Osaka, Japan); H3K9 trimethylation (Millipore, Billerica, MA); or H3K27 trimethylation (Millipore, Billerica, MA), overnight at 4°C. The immuno-complex was collected by Dynabeads Protein A (Invitrogen, Carlsbad, CA), and DNA was recovered with RNaseA treatment, Proteinase K treatment and isopropanol precipitation. Immunoprecipitated DNA was dissolved in 50 μl of 1× TE and 1 μl was used for quantitative PCR. Quantitative PCR was performed as described previously (Nakajima et al., 2009). IL-1β, F; 5′-TCC ACC ACG ATG ACA CAC TT-3′, R; 5′-GGG AGA AGC TTG ATG GGA AT-3′, NeuroD, F; 5′-GCA TGC ACG GGC TGA ACG C-3′, R; 5′-GGG ATG CAC CGG GAA GGA AG-3′.

Pregnant C57BL/6J mice were used to prepare NSCs. NSCs were obtained from whole brain of E14.5 mice and cultured. Briefly, the brain were triturated in serum-free medium: Dulbecco's modified Eagle's medium with 4500 mg/L glucose, 5 μg/ml insulin, 10 ng/ml EGF, 50 μg/ml transferrin, 10 ng/ml biotin, and 30 nM Na_2SeO_3. EGF (10 ng/ml) was used to keep the cultures proliferating. For differentiation experiments, ~10 neurospheres of the same size were isolated with a pipette and deposited on 10 μg/ml laminin-coated glass slides with 400 μl of serum-free medium with 10 ng/ml EGF. The NSCs were incubated overnight in medium containing EGF, which was then replaced by medium without EGF but containing IL-1β (10, 100 ng/ml) for 7 days. Differentiated neurospheres were fixed with 4% paraformaldehyde for 20 min at room temperature and processed for immunocytochemistry (ICC). The samples were rinsed with PBS twice and pretreated with PBS containing 0.3% Triton-X100 for 5 min at room temperature for ICC. After blocking in blocking buffer (PBS containing 5% FBS and 0.3% TritonX) for 1 h at room temperature, the samples were incubated at 4°C overnight with the following antibodies: antiβIII-tubulin (mouse IgG, 1:1000, Sigma-Aldrich, St. Louis, MO, T8660) After three washes with PBS, the samples were incubated for 1 h at room temperature with secondary antibodies conjugated with Alexa488 (Invi-

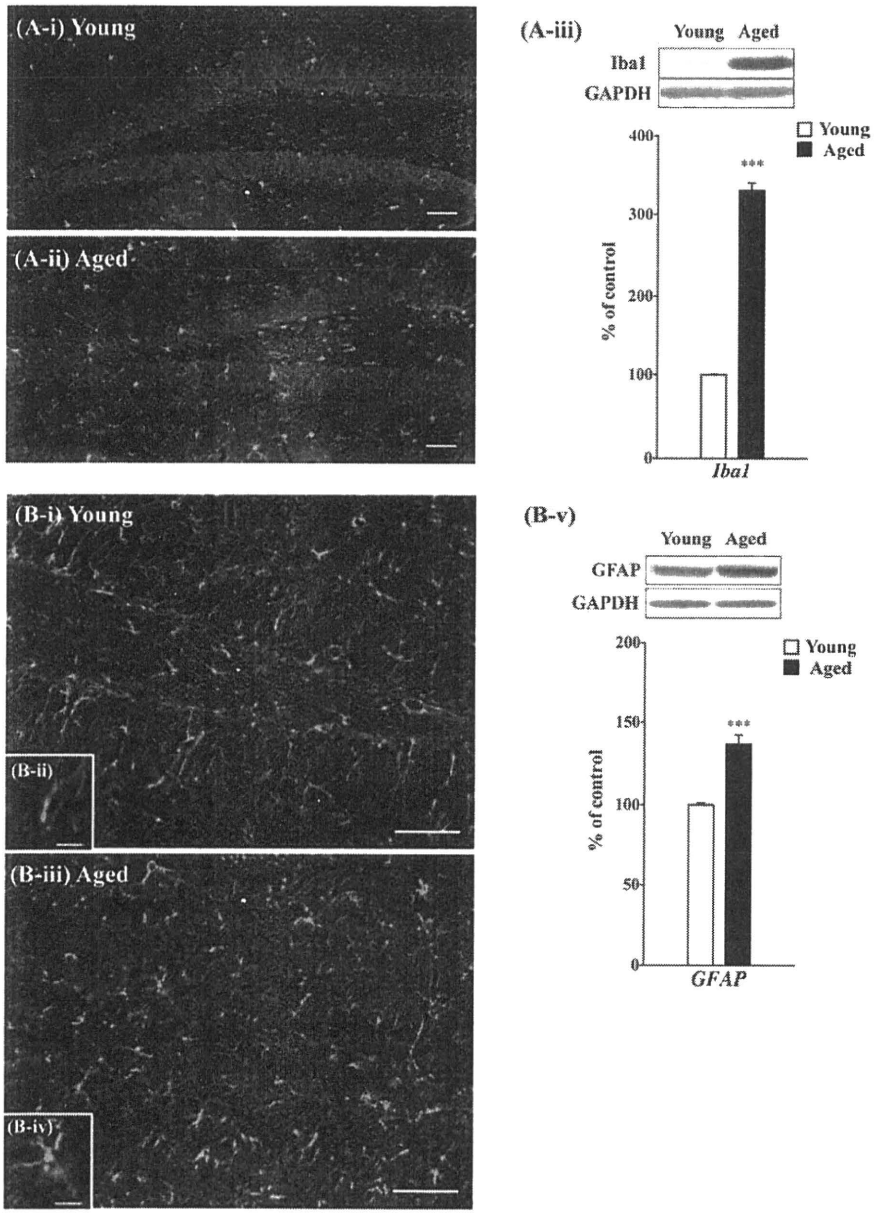

Fig. 1. **A**: Immunofluorescent staining for ionized calcium-binding adaptor molecule 1 (Iba1) in the dentate gyrus (DG) in young and aged mice. Iba1-like IR in the DG of aged mice (A-ii) was increased compared to that in young mice (A-i). Scale bar: 50 μm. (A-iii) *Upper*: Representative Western blot of Iba1. *Lower*: Changes in IR for Iba1 in the cytosolic fraction of hippocampus obtained from aged mice. Each column represents the mean ± SEM of six samples (***$P < 0.001$ vs. young group). **B**: Immunofluorescent staining for glial fibrillary acidic protein (GFAP) in the DG in young and aged mice. GFAP-like IR in the DG of aged mice (B-iii, B-iv: high magnification) was increased compared to that in young mice (B-i, B-ii: high magnification). Scale bar: 50 μm (B-i,-iii). Scale bar: 10 μm (B-ii, iv). (B-v) *Upper*: Representative Western blot of GFAP. *Lower*: Changes in IR for GFAP in the membranous fraction of hippocampus obtained from aged mice. Each column represents the mean ± SEM of 6 samples (***$P < 0.001$ vs. young group).

trogen, Carlsbad, CA) After being washed with PBS, the samples were mounted on slides and examined with microscope with a 10× objective lens (IX 71, Olympus, CO, Tokyo, Japan) and photographed with a digital camera (VB-6000, Keyence, CO, Osaka, Japan).

NSCs (5×10^5 cells per well) were treated with IL-1β (10 ng/ml, 100 ng/ml) for 8 h in 96-well plates. Afterward, the numbers of viable cells in culture were determined using the CellTiter-Glo Luminescent Cell Viability Assay kit (Promega, Madison, WI), which

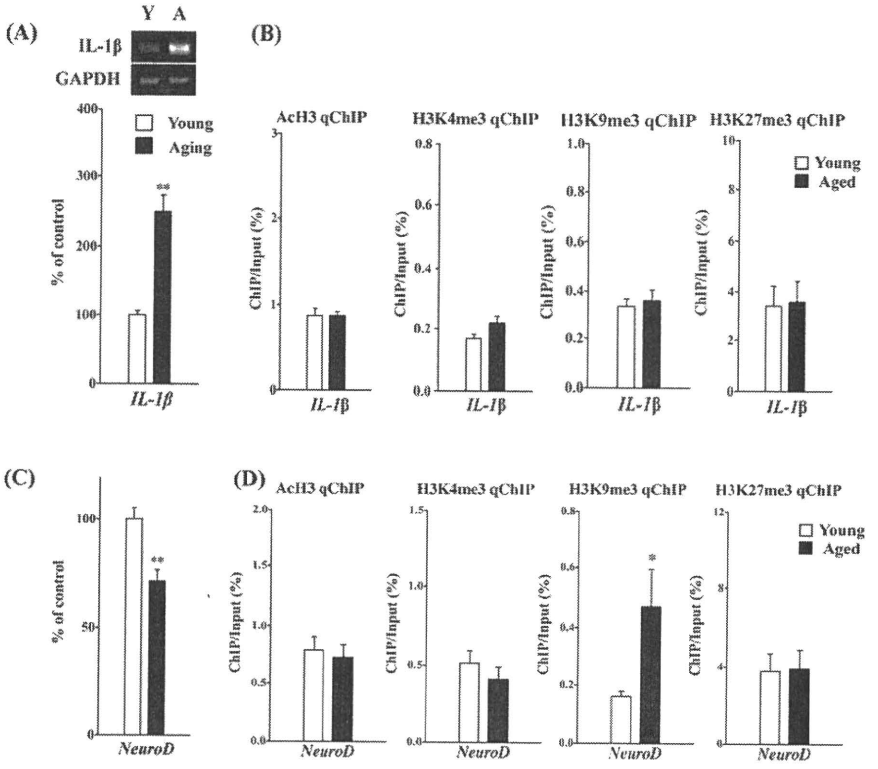

Fig. 2. **A**: *Upper*: Representative RT-PCR for IL-1β mRNA in the hippocampus obtained from young and aged mice. *Lower*: The intensity of the bands was semi-quantified using NIH Image software. The value for mRNA was normalized by that for the internal standard glyceraldehyde-3-phosphate dehydrogenase (GAPDH) mRNA. The value for aged mice is expressed as a percentage of the increase in young mice. Each column represents the mean ± SEM of three samples. (**$P < 0.01$ vs. young group). **B**: qChIP analysis of acetylated histone 3 (AcH3), histone 3 trimethylated at lysine 4 (H3K4me3), lysine 9 (H3K9me3), and lysine 27 (H3K27me3) at IL-1β loci in the hippocampus obtained from young and aged mice. Each column represents the mean ± SEM of three samples. **C**: Quantitative analysis of NeuroD mRNA in the hippocampus obtained from young and aged mice. Each column represents the mean ± SEM of 3 samples. (**$P < 0.01$ vs. the young group). **D**: qChIP analysis of AcH3, H3K4me3, H3K9me3 and H3K27me3 at NeuroD loci in the hippocampus obtained from young and aged mice. Each column represents the mean ± SEM of six samples (*$P < 0.05$ vs. young group).

evaluates the presence of ATP, an indicator of metabolically active cells, according to the manufacturer's instructions. All experiments were performed in triplicate wells.

The data are expressed as the mean ± SEM The statistical significance of differences between groups was assessed with Student's *t*-test (comparison of two groups) or an analysis of variance (ANOVA) followed by the Bonferroni test (comparison among multiple groups). A level of probability of 0.05 or less was considered significant.

To investigate a possible change in glial cell activity in the hippocampus of aged mice, immunohistochemical studies were performed. As shown in Figure 1A, the immunoreactivity (IR) of the specific microglial marker Iba1 was prominently observed in the DG of young mice (Fig. 1A-i). In the DG of aged mice, Iba1-IR was dramatically increased compared with that in young mice (Fig. 1A-ii). Western blots showed that the levels of Iba1 were significantly increased in the hippocampus of aged mice compared with those in young mice ($P < 0.001$; Fig. 1A-iii). Astrocytes in the DG of the hippocampus were stained with GFAP antibody. These astrocytes were sparsely distributed in young mice (Fig. 1B-i). In the DG of aged mice, IR for GFAP was increased compared with that in young mice (Fig. 1B-iii). Each individual astrocyte labeled by GFAP was hypertrophied with an enlarged cell body (Fig. 1B-ii and iv). Western blots showed that the level of GFAP was significantly increased in the hippocampus of aged mice compared with that in young mice ($P < 0.001$; Fig. 1B-v).

We next investigated the changes in the mRNA expression of IL-1β in the mouse hippocampus of young and aged mice. The mRNA expression of IL-1β was significantly increased in the hippocampus of aged mice compared with that in young mice ($P < 0.01$; Fig. 2A). To gain further insight into these phenomena, we next studied the histone modifications at the promoter regions of the IL-1β gene (Fig. 2B). As a

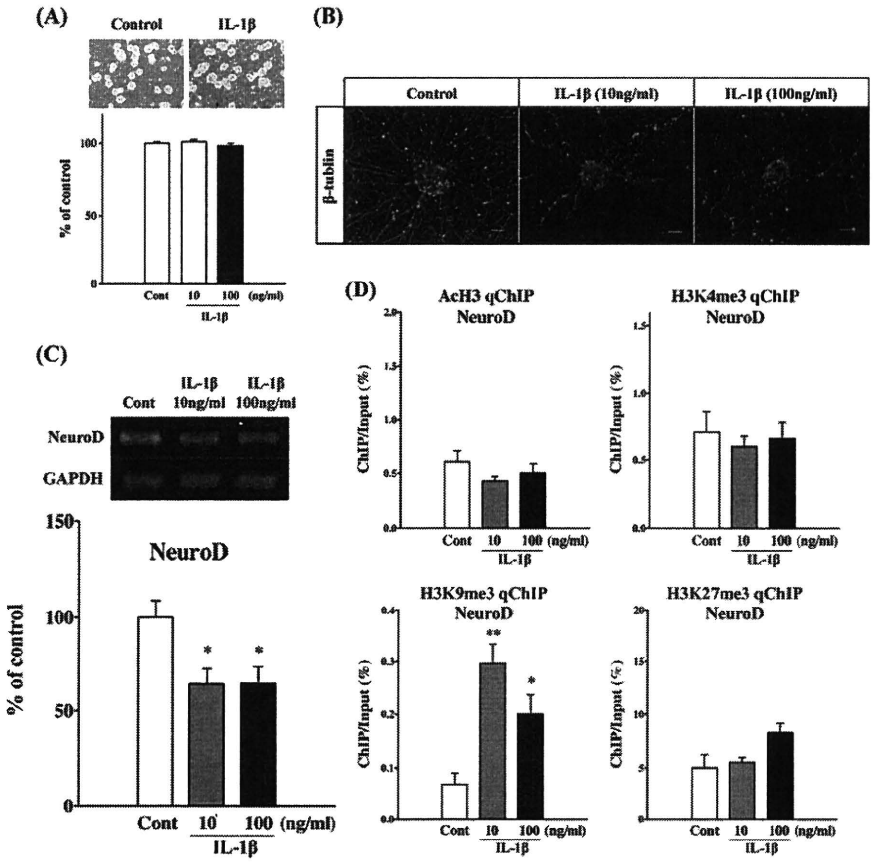

Fig. 3. **A**: Cell viability of neural stem cells after 1 day in the presence of 10 or 100 ng/ml IL-1β. Note that the IL-1β concentration has no effect on the survival of neural stem cells as indicated by Cell viability assay. **B**: Effects of IL-1β on the differentiation of neural stem cells into β-tubulin-positive neurons. The cells were incubated overnight in medium containing epidermal growth factor (EGF) that was replaced with medium alone or medium containing IL-1β (10, 100 ng/ml). Treatment with 10 or 100 ng/ml IL-1β decreased β-tubulin-positive neurons when compared with control cultures. **C**: *Upper*: Representative RT-PCR for NeuroD mRNA in neural stem cells. *Lower*: The intensity of the bands was semi-quantified using NIH Image software. The value for mRNA was normalized by that for the internal standard GAPDH mRNA. Each column represents the mean ± SEM of three samples. (*$P < 0.05$ vs. control group). **D**: qChIP analysis of AcH3, H3K4me3, H3K9me3, and H3K27me3 at NeuroD loci in neural stem cells incubated with IL-1β compared to that in control groups. The value for ChIP/Input was normalized by that for the internal standard in each control. Each column represents the mean ± SEM of 3 samples (*$P < 0.05$, **$P < 0.01$ vs. control group).

result, we detected no changes in two active histone modifications (acetylation of histone H3: AcH3, and trimethylation of lysine 4 on histone H3: H3K4) or in two repressive histone modifications (trimethylation of lysine 9 on histone H3: H3K9 and trimethylation of lysine 27 on histone H3: H3K27). Under these conditions, we found that mRNA expression of NeuroD, a neural progenitor cell marker, was significantly decreased in the hippocampus of aged mice compared with that in young mice ($P < 0.01$; Fig. 2C). In agreement with the PCR assay, we detected a significant increase in H3K9 trimethylation at the NeuroD promoter in the hippocampus of aged mice compared with that in young mice ($P < 0.05$; Fig. 2D). In contrast, we observed no changes in other histone modifications at the NeuroD gene promoter (Fig. 2D).

To further determine whether IL-1β could suppress neural stem cell proliferation and neural differentiation, we used neural stem cells prepared from whole brain of E14.5 mice. For the proliferation experiments, EGF (10 ng/ml) was used to keep the cultures proliferating. Under these conditions, treatment with IL-1β (1–100 ng/ml) failed to change the proliferation of neural stem cells as detected by a microtiter plate-based cell-survival assay (Fig. 3A). For the differentiation experiments, approximately 10 neurospheres of the same size were plated onto 10 μg/ml laminin-coated glass slides, and 400 μl of serum-free

medium with 10 ng/ml EGF was then added to each well. The neural stem cells were incubated overnight in medium with 10 ng/ml EGF and then replaced with medium alone or medium containing IL-1β (10–100 ng/ml). Treatment with IL-1β for 7 days produced a significant decrease in IR for the differentiated neural cell marker βIII-tubulin (Fig. 3B).

Under this condition, we next investigated the effects of treatment with IL-1β in neural stem cells on NeuroD mRNA expression in neural progenitor cells. Treatment with IL-1β significantly decreased the mRNA expression of NeuroD ($P < 0.05$; Fig. 3C). We next studied histone modifications at the NeuroD promoter. In agreement with the results in the aged brain, we found a significant increase in H3K9 trimethylation at the NeuroD promoter in neural stem cells that had been incubated with IL-1β compared to that in control groups ($P < 0.05$, $P < 0.01$; Fig. 3D).

Microglia constantly survey the microenvironment for noxious agents or injurious processes (Nimmerjahn et al., 2005). With aging, microglia are thought to increase in number and become activated, and may enter a phagocytic or reactive stage (Lucin and Wyss-Coray, 2009). In this study, Iba1-positive microglia were significantly increased in the DG of the hippocampus of aged mice.

Based on the activation stimuli, microglia are informed of the encountered problem and instructed to act in an appropriate manner and perform a defined task. If the disturbance is relatively minor, microglia may secrete anti-inflammatory cytokines and supportive growth factors (Lucin and Wyss-Coray, 2009). If the disturbance poses a serious threat, such as a pathogen invasion, microglia may release toxic factors to kill the pathogen and recruit help by releasing proinflammatory cytokines. If we consider the continuum of potential microglial responses, how a given insult is interpreted can mean the difference between a beneficial outcome or a detrimental outcome if the response is either too aggressive or too passive.

As well as microglia, aging caused a dramatic increase in GFAP-positive IR that is located in dendritic astrocytes, with an expanding distribution in the hippocampus of aged mice. Each individual astrocyte labeled by GFAP was branched, which indicates the activation of astrocytes in the hippocampus of aged mice. This notion is supported by a previous finding that in humans the GFAP level increases dramatically after the age of 65 years, and more specifically in the hippocampal formation (David et al., 1997). Furthermore, aging had a differential effects on astrocytic and microglial hyperactivity in gray vs. white matter areas. This mosaic of glial aging suggests that multiple mechanisms are at work during aging.

The activation of microglia or astrocytes that secrete and express numerous regulatory ligands can affect cells of immune or nonimmune tissues, such as neurons through the release of cytokines and chemokines. Cytokines and chemokines have been classified as molecules that coordinate inflammatory and immune responses, and also mediate normal, ongoing signaling between cells of nonimmune tissues (Bodles and Barger, 2004). In this study, the mRNA level of IL-1β in the hippocampus was significantly increased by aging. This result is partly supported by previous findings (Murray and Lynch, 1998).

Epigenetic alterations of DNA play key roles in determining gene structure and expression (Jaenisch and Bird, 2003; Tsankova et al., 2007). A major epigenetic modification, chromatin remodeling, modulates gene expression with high temporal and spatial resolution by permitting small groups of nucleosomes to become more or less open, which consequently enhances or inhibits access of the transcriptional machinery to specific promoter regions. The acetylation and methylation of histone proteins at specific residues play a major role in chromatin remodeling. Lysine acetylation almost always correlates with chromatin accessibility and transcriptional activity, whereas lysine methylation can have different effects depending on which residue is modified (Jenuwein and Allis, 2001). Trimethylation of H3K4 is associated with transcribed chromatin (Li et al., 2007). In contrast, trimethylation of H3K9 and H3K27 generally correlates with repression (Bernstein et al., 2005). In this study, aging did not cause any changes in the acetylation or methylation of histone proteins at any genes of IL-1β. Gene expression has been considered to be mediated through the complex machinery, which is regulated in a coordinated manner by transcription factors, protein kinases and cotranscriptional factors, which are classified as epigenetic modulators. Thus, gene transcription can be controlled by transcriptional factors singly or in combination with other transcriptional factor and protein kinases (Wang et al., 2009). With regard to such complex machinery, we hypothesize that the increased expression of IL-1β mRNA observed in the hippocampus of aged mice may be modulated by activated transcription factors with or without protein kinases, other than epigenetic modifications.

We previously reported that aging decreased the expression of the migrated neural progenitor doublecortin in association with a significant decrease in H3K4 trimethylation and a significant increase in H3K27 trimethylation in the hippocampus (Kuzumaki et al., 2010). In this study, we found that aging induced a significant increase in H3K9 trimethylation at the promoter of another neural progenitor cell marker (NeuroD) in the hippocampus. These findings suggest that aging causes the epigenetically repressive modulation of neural progenitors in the hippocampus.

We finally investigated whether IL-1β could affect neural progenitor cells through epigenetic regulation. In vitro treatment of neural stem cells prepared from whole brain of E14.5 mice with IL-1β significantly increased H3K9 trimethylation at the NeuroD promoter. These findings suggest that IL-1β, which may be produced by aging, decreases neural progenitor cells through epigenetic modulation. It has been reported that IL-1β suppresses the proliferation of hippocampal progenitor cells (Koo and Duman, 2008). It has generally been accepted that the decreased proliferation of neural stem cells is responsible for decreased neural differentiation, and increased prolifiration could correspond to the promotion of neurogenesis. In this study, treatment with 10–100 ng/ml of IL-1β produced a significant decrease in neural differentiation with no change in the proliferation of neural stem cells. This apparent discrepancy may be the result of the relatively short exposure time to IL-1β in the present cell survival assay. However, we can not deny the possibility that epigenetic modification at the NeuroD promoter by IL-1β may lead to a direct change in the neurogenesis/gliogenesis ratio or that IL-1β may promote neural differentiation from neural stem cells without affecting the survival/proliferation of neural stem cells via "unknown pathways."

In conclusion, this study demonstrated that microglia and astrocytes were activated in the DG of the hippocampus of aged mice. Furthermore, aging significantly increased mRNA levels of IL-1β without related histone modifications and increased H3K9 trimethylation at the promoter of a neural progenitor cell marker (NeuroD) in the hippocampus of aged mice. Moreover, in vitro treatment of neural stem cells prepared from whole brain of E14.5 mice with IL-1β significantly increased H3K9 trimethylation at the NeuroD promoter. These findings suggest that aging may activate microglia and astrocytes with an increased expression of IL-1β in the hippocampus. Furthermore, increased IL-1β could lead to a decrease in hippocampal neurogenesis via epigenetic modifications.

REFERENCES

Bernstein BE, Kamal M, Lindblad-Toh K, Bekiranov S, Bailey DK, Huebert DJ, McMahon S, Karlsson EK, Kulbokas EJ III, Gingeras TR, Schreiber SL, Lander ES. 2005. Genomic maps and comparative analysis of histone modifications in human and mouse. Cell 120:169–181.

Bodles AM, Barger SW. 2004. Cytokines and the aging brain–what we don't know might help us. Trends Neurosci 27:621–626.

David JP, Ghozali F, Fallet-Bianco C, Wattez A, Delaine S, Boniface B, Di Menza C, Delacourte A. 1997 Glial reaction in the hippocampal formation is highly correlated with aging in human brain. Neurosci Lett 235:53–56.

Eriksson PS, Perfilieva E, Bjork-Eriksson T, Alborn AM, Nordborg C, Peterson DA, Gage FH. 1998. Neurogenesis in the adult human hippocampus. Nat Med 4:1313–1317.

Jaenisch R, Bird A. 2003. Epigenetic regulation of gene expression: how the genome integrates intrinsic and environmental signals. Nat Genet 33 Suppl:245–254.

Jenuwein T, Allis CD. 2001. Translating the histone code. Science 293:1074–1080.

Koo JW, Duman RS. 2008. IL-1beta is an essential mediator of the antineurogenic and anhedonic effects of stress. Proc Natl Acad Sci USA 105:751–756.

Kuhn HG, Dickinson-Anson H, Gage FH. 1996. Neurogenesis in the dentate gyrus of the adult rat: age-related decrease of neuronal progenitor proliferation. J Neurosci 16:2027–2033.

Kuzumaki N, Ikegami D, Tamura R, Sasaki T, Niikura K, Narita M, Miyashita K, Imai S, Takeshima H, Ando T, Igarashi K, Kanno J, Ushijima T, Suzuki T, Narita M. 2010. Hippocampal epigenetic modification at the doublecortin gene is involved in the impairment of neurogenesis with aging. Synapse (in press).

Li B, Carey M, Workman JL. 2007. The role of chromatin during transcription. Cell 128:707–719.

Lucin KM, Wyss-Coray T. 2009. Immune activation in brain aging and neurodegeneration: Too much or too little? Neuron 64: 110–122.

Murray CA, Lynch MA. 1998. Evidence that increased hippocampal expression of the cytokine interleukin-1 beta is a common trigger for age- and stress-induced impairments in long-term potentiation. J Neurosci 18:2974–2981.

Nakajima T, Yamashita S, Maekita T, Niwa T, Nakazawa K, Ushijima T. 2009. The presence of a methylation fingerprint of Helicobacter pylori infection in human gastric mucosae. Int J Cancer 124:905–910.

Nimmerjahn A, Kirchhoff F, Helmchen F. 2005. Resting microglial cells are highly dynamic surveillants of brain parenchyma in vivo. Science 308:1314–1318.

Takeshima H, Yamashita S, Shimazu T, Niwa T, Ushijima T. 2009. The presence of RNA polymerase II, active or stalled, predicts epigenetic fate of promoter CpG islands. Genome Res 19:1974–1982.

Tsankova NM, Kumar A, Nestler EJ. 2004. Histone modifications at gene promoter regions in rat hippocampus after acute and chronic electroconvulsive seizures. J Neurosci 24:5603–5610.

Tsankova N, Renthal W, Kumar A, Nestler EJ. 2007. Epigenetic regulation in psychiatric disorders. Nat Rev Neurosci 8:355–367.

Wang K, Saito M, Bisikirska BC, Alvarez MJ, Lim WK, Rajbhandari P, Shen Q, Nemenman I, Basso K, Margolin AA, Klein U, Dalla-Favera R, Califano A. 2009. Genome-wide identification of post-translational modulators of transcription factor activity in human B cells. Nat Biotechnol 27:829–839.

Bull. Natl. Inst. Health Sci., **128**, 58-64 (2010) **Original**

臭素化難燃剤hexabromocyclododecane（HBCD）のラット周産期暴露における発達期免疫機能影響について

蜂須賀暁子#，中村亮介，佐藤雄嗣，中村里香，渋谷 淳，手島玲子

Effects of perinatal exposure to the brominated flame-retardant hexabromocyclododecane (HBCD) on the developing immune system in rats

Akiko Hachisuka#, Ryosuke Nakamura, Yuji Sato, Rika Nakamura, Makoto Shibutani, Reiko Teshima

To evaluate the developmental immunotoxicity of brominated flame retardant, hexabromocyclododecane (HBCD), maternal Sprague-Dawley rats were given HBCD at dietary concentrations of 0, 100, 1000, 10000 ppm from gestational day 10 to postnatal day 21 (postnatal week 3, PNW3). At PNW3 and PNW11, lymphocytes in the spleen, thymus, and peripheral blood of male pups were subjected to flow cytometric analyses for expression of surface markers (CD3, CD4, CD8a, CD25, CD45RA, CD71, and CD161 (NKRP1A)). The spleen and thymus weights, and number of white blood cells of two organs did not change between HBCD-exposed and control groups at PNW3 and PNW11. A significant decrease in thyroid hormone T3 and increase in serum albumin concentration were observed at PNW3 and lasted until PNW11. By flow cytometric analysis, the dramatic change was not observed in the population of the splenic and thymic T/B lymphocyte between the HBCD treated groups and control group. In the peripheral blood of BNW3 rats, the population of activated T cells was decreased and that of inactivated B cells was increased. And the population of NK cells in the spleen was decreased. All of these changes were mild in degree, and returned to the normal levels by PNW11. Production of anti-KLH IgG antibody after KLH immunization was reduced by the 10000 ppm HBCD treatment. These results suggest that developmental exposure to the highest dose of HBCD had a weak immunomodulatory effect at PNW3, and most of the immunomodulatory effect had recovered to normal levels by PNW11.

Keywords: hexabromocyclododecane, brominated flame retardant, rat, immunotoxicity, developmental toxicity

1．はじめに

難燃剤とは，プラスチック・ゴム・繊維・紙・木材などの可燃性の素材に添加してそれらを燃えにくくし，あるいは炎が広がらないようにする化合物であり，ハロゲン化合物などの有機系，金属水酸化物などの無機系に分類される．Hexabromocyclododecane（HBCD）は，ハロゲン系難燃剤の中でも臭素含有率が高いことから，少量で優れた難燃機能を有するとされ，日本において年間約3,000トンの需要量があり，その約８割が建設用の発泡系断熱材に，約２割がカーテンなどの繊維製品に利用されている．難分解性，高蓄積性であることから2004年９月化審法の第一種監視化学物質に指定された．長期毒性については不明な点が多いが，2008年Ema[1]らの２世代生殖毒性試験によりヒトに対する毒性は高くないと判断され，2009年５月の改正においても第一種監視化学物質のまま据え置かれている．

他方，免疫系は環境化学物質や薬物の有害影響に鋭敏に反応し，かつその健康影響はアレルギー，感染症，発がんなど多様な形で発現することが知られ，環境因子の影響を評価する際の重要な指標であることが指摘されてきた．また，胎児期から小児期にかけては生体組織・機

#To whom correspondence should be addressed:
Akiko Hachisuk; 1-18-1 Kamiyoga, Setagaya-ku, Tokyo 158-8501, Japan; Tel: +81-3-3700-1141 ext. 243; Fax: +81-3-3707-6950; E-mail: hachisuk@nihs.go.jp

能が発育段階にあり未熟であるために環境有害因子に対して感受性が高い時期（critical window）と考えられており，胎児期から小児期に受けた影響は生涯にわたって続く障害となる場合が少なくない．以上の点から，化学物質の発達期暴露による免疫影響についての検討は極めて重要なものであるが，一般毒性試験の中では実施されていないことから，免疫毒性試験評価手法の高度化，標準化が，国際的にも望まれている．

本報告では，対象化合物として本邦で使用頻度の高い臭素系難燃剤を取り上げ，胎児期から幼児期にかけてのラットに暴露した際の，胸腺，脾臓を中心にした免疫機能影響の評価研究を行った．HBCDを含むtetrabromobisphenol A（TBBPA），decabromodiphenyl ether（DBDE）等の臭素系難燃剤は，甲状腺機能阻害を有することが示唆されている化学物質でもある[2]．そこで，免疫影響について考察するにあたっては，甲状腺機能障害性についても考慮した．最後に，HBCDの免疫影響について，すでに報告したDBDEの免疫影響[3]との比較を加えた．

2．方法

動物は，各群10匹ずつの妊娠SD：IGSラットを用い，妊娠10日目から出産３週目まで，被験物質であるHBCDを，100ppm，1000ppm，10000 ppmの濃度で餌（大豆除去飼料（西川食））に混ぜ，親に自由摂取させた．大豆イソフラボンは代表的な植物エストロゲンであり，甲状腺ペルオキシダーゼの活性阻害作用によりヨウ素欠乏状態で甲状腺機能低下を来すとの報告があるため[4]，本実験では大豆成分の影響を避けるために被験物質投与期間は大豆除去食とした．出産３週目（PNW3）に離乳を行い，各群雌雄10匹ずつの児ラットの解剖を行なった．残りの児ラットについては，３週目からは，通常のCRF-1飼料を与えて11週まで飼育し，回復の程度を見る実験に供した．３週目，11週目の解剖時の免疫影響評価のための項目は，表１に示した通りである．病理組織学的検査のみ雌雄児ラットについて行い，他は雄児ラットについて行った．

(1)　血液学的検査：末梢血白血球数は，ラット後大動脈より採血した血液20μlをあらかじめ80μlの0.5% EDTA-2K溶液が入った1.5mlチューブに入れて混和し，多項目自動血球計数装置（M-2000，Sysmex corp）に供した．赤血球数（RBC），白血球数（WBC），血小板数（PLT），ヘモグロビン濃度（HGB），ヘマトクリット値（HCT），平均赤血球容積（MCV）平均赤血球血色素量（MCH）及び平均赤血球血色素濃度（MCHC）の測定を行なった．白血球百分比は，Wright染色した塗沫標本を作製し，杆状核好中球（Band），分葉核好中球（Seg），好酸球（Eosino），好塩基球（Baso），リンパ球（Lympho），単球（Mono）及び有核赤血球（Ebl）について血液細胞自動分析装置（Microx MEG50S, Sysmex）を用いて計測した．

表１　本実験で用いた免疫毒性のマーカー

(1)	末梢血白血球数，白血球百分比
(2)	胸腺，脾臓の重量
(3)	胸腺，脾臓の病理組織学的検査
(4)	体液性免疫： KLHに対する血中IgM, IgG抗体産生（ELISA） 脾臓，末梢血，リンパ節のフローサイトメトリー：B細胞数（CD45RA）
(5)	細胞性免疫 脾臓，末梢血，リンパ節のフローサイトメトリー：T細胞数（CD3）及び T細胞サブセット（CD4及びCD8a），調節性T細胞（CD4+CD25+）， 活性化T細胞（CD3+CD71+）
(6)	非特異的免疫 脾臓，末梢血のNK細胞数

(2)　胸腺，脾臓の重量：採血終了後，動物を放血死させ，免疫系器官である胸腺，脾臓の重量を測定した．重量測定後，臓器を２つにわけ，一方を病理組織学的検査用とし，残りをフローサイトメトリー用に供した．

(3)　病理組織学的検査：上記(2)で記した胸腺，脾臓の１部を，常法に従って中性緩衝ホルマリン液で固定を行い，薄切切片を作成し，ヘマトキシリン・エオジン染色を施した．

(4)　体液性免疫：抗体産生への影響を調べるために，解剖に供した児ラットとは別個体雄児ラットに，生後（PND）23日，33日及び43日にKLH（keyhole limpet hemocyanin）50μgをalum 1mgとともに腹腔内投与し，40及び50日目に採血し，500～500,000倍希釈し，KLHを固相抗原としたELISAにて，KLH特異的IgG及びIgM抗体価を測定した[5]．また，脾臓，末梢血，血液中Bリンパ球の割合を，PECy5標識抗CD45RA抗体処理によるフローサイトメトリーを用いて解析した．

(5)　細胞性免疫：細胞性免疫に関与する胸腺，脾臓，末梢血中Tリンパ球の割合の解析のため，フローサイトメトリーによる解析を行なった．全T細胞数は，FITC標識抗CD3抗体を用い，CD4，CD8 T細胞サブセットは，PECy5標識抗CD4抗体及びPE標識抗CD8a抗体を用い，調節性T細胞（CD4+CD25+）[6]については，PE標識抗CD25抗体を併用し，活性化T細胞（CD3+CD71+）については，PE標識抗CD71（トランスフェリン受容体）抗体を併用して解析を行なった[7]．

(6)　非特異的免疫：脾臓，末梢血中のNK細胞数の割合をFITC標識抗NKRP1A（CD161）抗体を用いてフローサイトメトリーで解析した．

(7)　フローサイトメトリー：上記(4)-(6)で示したリン

パ球サブポピュレーション解析は，脾臓，胸腺，末梢血細胞を３種の蛍光で標識した抗体を用い三重染色後，Facs Caliber（Becton Dickinson）を用いて行なった．動物実験は研究所の規定に準拠し，実験動物委員会の承認に基づき実施した．

３．研究結果

(1) HBCDの免疫担当細胞への影響

図１に，臭素化難燃剤HBCD親ラット投与による児雄ラットの体重，臓器重量変化の結果を示す．３週令時，11週令時共に，HBCD 100，1000，10000ppm投与群で対照群と比較して，体重，脾臓，胸腺重量に有意な差はみられなかった．なお，母動物の体重にも投与による影響は認められなかった．また，HBCD投与ラットの脾臓，胸腺細胞の白血球数についても，有意差はみられなかった．なお，肝臓重量は，1000, 10000ppm投与群の３週令において，有意な増加が認められたが，11週令においては，有意差は認められなかった．

次に表２，表３に，３週令ラットと11週令ラットの血液学的検査を行なった結果を示すが，末梢血白血球数（表２），白血球百分比（表３）ともに，３週令，11週令ラットにおいて，対照と比べて有意な変化はみられなかった．なお，３週令で，赤血球容積，11週令で血色素濃度の用量依存的な上昇が観察され（表２），また，３週令で，有核赤血球（Ebl）のわずかな上昇傾向がみられた（表３）．

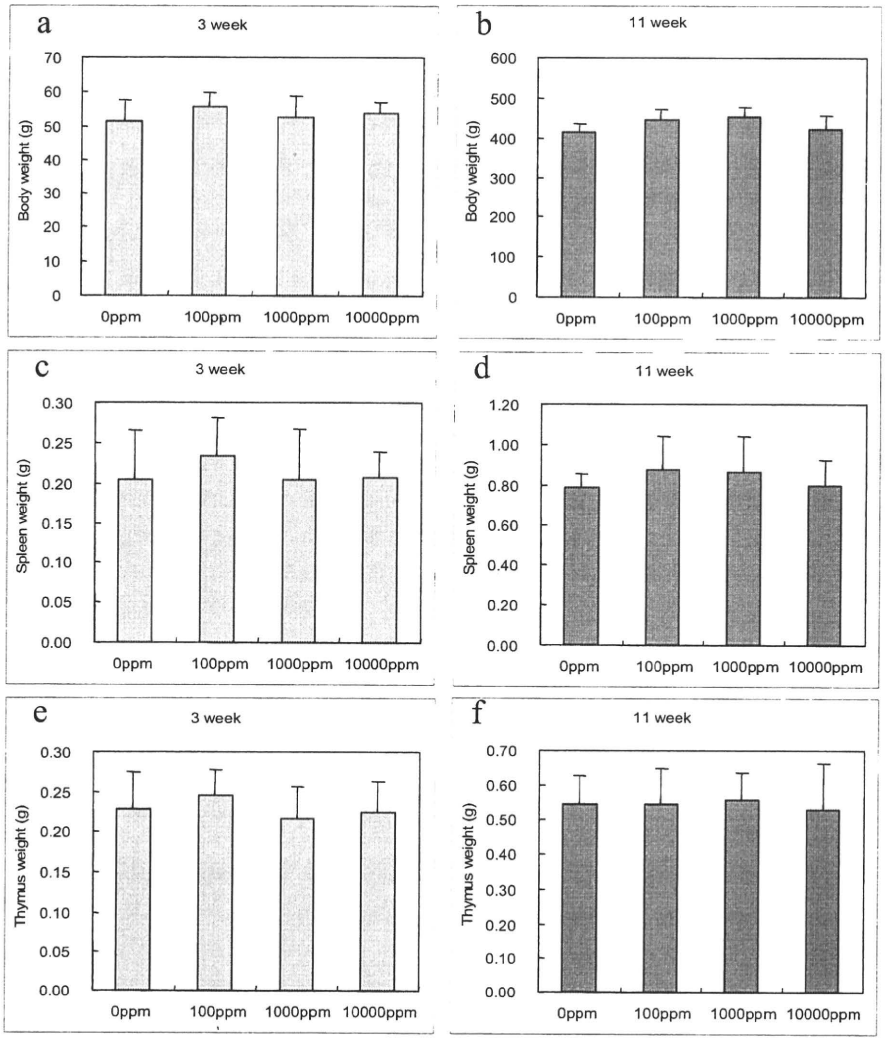

Fig. 1 Effect of perinatal exposure to HBCD on the body weight and the immune-related organs weight of offspring
Dams were fed *ad lib* HBCD-containing diet from gestational day 10 to PNW3. The body weight (a, b), spleen wight (c, d), and thymus weight (e, f) of the male offspring at PNW3 and PNW11, respectively. Means (n=10) ± SD are shown. There was no significant difference (Dunnett, $p<0.05$).

次いで，フローサイトメトリーによるリンパ球ポピュレーションの解析では，HBCD投与群と対照群との間に幾つかの項目で，リンパ球サブポピュレーションにおける変化が観察された．表４に，５%以上の有意差を持って変化のみられた項目につき，解析したリンパ球サブポピュレーションの割合を数値で表したものを示した．T細胞のサブポピュレーション解析では，脾臓リンパ球において，HBCD 100ppm, 10000ppm投与11週令時で，CD8+ T細胞の上昇が認められた．また，末梢血における活性化T細胞の割合の低下，並びに非活性化B細胞の

Table 2 Hematological changes in male rats perinatally exposed to HBCD

group	WBC	RBC	HGB	HCT	MCV	MCH	MCHC	PLT	
PNW 3	x 10^2/ul	x 10^4/ul	g/dl	%	fL	pg	g/dL	x 10^4/ul	n
M-1 (control)	35.3 ± 11.3	327.7 ± 22.7	5.19 ± 0.69	20.00 ± 1.81	61.05 ± 4.23	15.85 ± 1.90	25.92 ± 1.93	118.92 ± 19.50	10
M-2 (HBCD 100 ppm)	30.9 ± 10.0	336.8 ± 30.2	5.83 ± 0.87	21.59 ± 1.85	64.25 ± 4.31	17.32 ± 2.32	26.85 ± 2.33	121.77 ± 11.28	10
M-3 (HBCD 1000 ppm)	47.5 ± 11.8 *	328.1 ± 24.0	5.76 ± 0.73	21.16 ± 2.07	64.50 ± 4.27	17.55 ± 1.77	27.17 ± 1.19	128.38 ± 11.06	10
M-4 (HBCD 1000 ppm)	39.6 ± 7.9	322.3 ± 23.7	5.98 ± 1.18	21.57 ± 3.24	66.71 ± 6.26 *	18.46 ± 2.67 *	27.55 ± 1.94	123.99 ± 22.54	10
PNW11									
M-1 (control)	82.1 ± 17.8	758.6 ± 63.6	14.27 ± 1.93	46.74 ± 3.79	61.64 ± 1.63	18.78 ± 2.01	30.49 ± 3.29	108.85 ± 9.88	10
M-2 (HBCD 100 ppm)	109.8 ± 30.8 *	786.5 ± 30.4	15.60 ± 0.59	48.03 ± 1.79	61.07 ± 1.23	19.85 ± 0.32	32.47 ± 0.50	111.32 ± 12.15	10
M-3 (HBCD 1000 ppm)	110.0 ± 29.3 *	815.1 ± 55.3 *	15.96 ± 0.82 *	49.29 ± 3.32	60.48 ± 1.16	19.59 ± 0.50	32.42 ± 0.82	117.26 ± 13.72	10
M-4 (HBCD 1000 ppm)	103.4 ± 34.1	766.4 ± 39.6	15.27 ± 0.56	46.42 ± 2.16	60.61 ± 1.30	19.94 ± 0.60	32.90 ± 0.46 *	123.97 ± 19.15 *	10

Values are mean ± SD of 10 rats. *<0.05 (Dunnett's-test)

Table 3 White blood cell classification in male rats perinatally exposed to HBCD

group	n	Lymp	Seg	Eosi	Mono	Band	Ebl
PNW3		%	%	%	%	%	n
M-1 (control)	9	78.88 ± 4.74	19.73 ± 4.77	0.61 ± 0.74	0.61 ± 0.49	0.0 ± 0.0	0.06 ± 0.17
M-2 (HBCD 100 ppm)	10	79.02 ± 3.18	19.63 ± 3.26	0.60 ± 0.46	0.75 ± 0.63	0.0 ± 0.0	0.48 ± 0.66
M-3 (HBCD 1000 ppm)	10	81.69 ± 3.81	17.21 ± 4.19	0.45 ± 0.37	0.65 ± 0.75	0.0 ± 0.0	0.26 ± 0.37
M-4 (HBCD 1000 ppm)	10	81.41 ± 4.06	17.42 ± 4.50	0.36 ± 0.50	0.81 ± 0.90	0.0 ± 0.0	1.00 ± 1.45
PNW11							
M-1 (control)	10	84.64 ± 5.46	13.51 ± 5.15	0.90 ± 0.94	0.95 ± 0.69	0.0 ± 0.0	0.05 ± 0.16
M-2 (HBCD 100 ppm)	10	84.27 ± 4.88	13.33 ± 4.67	1.50 ± 1.15	0.90 ± 0.70	0.0 ± 0.0	0.00 ± 0.00
M-3 (HBCD 1000 ppm)	10	87.56 ± 4.33	10.44 ± 3.79	1.05 ± 0.93	0.95 ± 0.64	0.0 ± 0.0	0.05 ± 0.16
M-4 (HBCD 1000 ppm)	10	86.44 ± 3.36	11.86 ± 3.34	0.75 ± 0.68	0.95 ± 0.50	0.0 ± 0.0	0.00 ± 0.00

Values are mean ± SD. There was no significant difference (Dunnett, $p<0.05$).

Table 4 Effects of HBCD on subpopulations of immune cells

T cell subpopulations

	Spleen3w				Spleen 11w				Note
HBCD:	0 ppm	100 ppm	1000 ppm	10000 ppm	0 ppm	100 ppm	1000 ppm	10000 ppm	
CD3(+) CD8a(+)	6.84 ± 1.3	8.15 ± 1.88	7.22 ± 1.52	6.6 ± 1.44	13.42 ± 2.71	18 ± 4.21*	15.2 ± 3.54	18.4 ± 4.58*	CD8 T cell
CD8a(+) CD4(−)	6.86 ± 0.95	8.12 ± 2.16	6.99 ± 1.42	6.43 ± 1.44	14.42 ± 2.23	18.54 ± 4.34*	16.85 ± 4.31	18.87 ± 4.82*	CD8

Activation of T/B cells

	Thymus 3w				Thymus 11w				Note
HBCD:	0 ppm	100 ppm	1000 ppm	10000 ppm	0 ppm	100 ppm	1000 ppm	10000 ppm	
CD3(+) CD71(+)	2.67 ± 0.87	2.46 ± 0.8	1.82 ± 0.55*	1.87 ± 1.15	0.92 ± 0.97	0.74 ± 0.51	1.02 ± 0.84	1.04 ± 0.7	active T cell
	Peripheral Blood 3w				Peripheral Blood 11w				Note
HBCD:	0 ppm	100 ppm	1000 ppm	10000 ppm	0 ppm	100 ppm	1000 ppm	10000 ppm	
CD3(+) CD71(+)	13.51 ± 3.47	14.01 ± 2.16	11.81 ± 1.96	10.4 ± 2.02*	1.45 ± 0.54	1.35 ± 0.6	1.27 ± 0.47	1.32 ± 0.24	active T cell
CD71(+) CD45RA(+)	20.79 ± 4.03	20.24 ± 2.97	23.08 ± 1.77	25.81 ± 2.84**	20.91 ± 5.79	19.65 ± 7.81	22.94 ± 6.7	21.22 ± 5.22	Inactive B cell

Treg, NK, NKT cells

	Spleen3w				Spleen 11w				Note
HBCD:	0 ppm	100 ppm	1000 ppm	10000 ppm	0 ppm	100 ppm	1000 ppm	10000 ppm	
NKRP1A(+) CD25(−)	11.36 ± 0.79	11.55 ± 1.19	11.25 ± 1.67	9.99 ± 1.11**	21.47 ± 2.47	21.47 ± 3.9	23.28 ± 4.29	20.77 ± 2.33	NK cell
NKRP1A(+) CD4(+)	6.47 ± 0.61	6.28 ± 0.81	6.4 ± 1.31	5.63 ± 0.81**	12.53 ± 1.88	12.89 ± 1.85	13.78 ± 2.66	13.09 ± 1.72	CD4NKT
NKRP1A(+) CD4(−)	5.75 ± 0.35	6.06 ± 1.09	5.65 ± 0.87	5.09 ± 0.76*	10.63 ± 1.63	9.97 ± 3.44	11.38 ± 2.47	9.44 ± 2.39	NK cell
	Thymus 3w				Thymus 11w				Note
HBCD:	0 ppm	100 ppm	1000 ppm	10000 ppm	0 ppm	100 ppm	1000 ppm	10000 ppm	
CD25(+) CD4(+)	7.7 ± 2.57	5.15 ± 0.94*	7.69 ± 1.27	7.85 ± 2.85	4.16 ± 1.09	3.98 ± 0.87	4.41 ± 0.76	4.32 ± 1.22	Treg
NKRP1A(+) CD4(−)	0.07 ± 0.03	0.07 ± 0.03	0.06 ± 0.02	0.07 ± 0.05	0.2 ± 0.04	0.2 ± 0.05	0.25 ± 0.09	0.27 ± 0.08*	NK cell
	Peripheral Blood 3w				Peripheral Blood 11w				Note
HBCD:	0 ppm	100 ppm	1000 ppm	10000 ppm	0 ppm	100 ppm	1000 ppm	10000 ppm	
NKRP1A(+) CD25(+)	0.12 ± 0.03	0.1 ± 0.03	0.09 ± 0.02	0.08 ± 0.04*	0.27 ± 0.07	0.23 ± 0.08	0.27 ± 0.07	0.25 ± 0.09	CD25NK

*$p<0.05$, **$p<0.01$

割合の上昇が，３週令時ラットHBCD 10000ppm投与群でみられた．さらに，NK細胞については，脾臓におけるNKRP1A（NK受容体）陽性細胞の割合の減少が，HBCD 10000ppm投与３週令ラットにおいて観察された．

HBCD投与による血液生化学的検査結果については，表５に示すが，３週令時10000ppmHBCD投与群において，甲状腺ホルモンT3の有意な減少及びTSHの有意な上昇が観察された．11週令時においてもT3の有意な低下が，1000，10000ppm HBCD投与群でみられた．また，血清のアルブミン値の上昇が，11週令時の10000ppmHBCD投与群において観察された．

病理組織学的所見を表６に示す．３週令雄の1000ppm HBCD投与群において，貪食したマクロファージであるstarry-sky像が増加していたが用量依存性は認められなかった．その他は，顕著な変化は認められなかった．

投与ラットのKLHに対する抗体産生への影響を図２に示す．図には，KLHで２回免疫したラットから得た血清（PND40）のELISAで測定したKLH特異的IgG抗体価とHBCDの用量依存性を調べた結果を示しているが，HBCDの濃度が上昇するにつれ，抗体価の減少する傾向が得られ，HBCD 10000ppm投与群で，対照群と比較して有意な抗体価の減少が観察された．

４．考察

臭素化難燃剤HBCDの胎児期及び幼児期投与による児

Table 5　Serum levels of thyroid-related hormones of the offspring perinatally exposed to HBCD

	HBCD in diet (ppm)													
	0				100			1000				10000				
PNW3																
No. of offspring examined	10				10			10				10				
T3 (ng/ml)	1.09	±	0.11	[a]	1.13	±	0.12	1.06	±	0.08		0.93	±	0.10	**	
T4 (ug/dl)	4.39	±	0.93		4.20	±	0.77	4.78	±	0.49		4.20	±	0.52		
TSH (ng/ml)	5.40	±	0.62		6.66	±	1.24	6.07	±	1.41		7.00	±	1.31	*	
A/G ratio	2.17	±	0.43		2.34	±	0.59	2.08	±	0.34		1.93	±	0.70	[b]	
albumin (g/dl)	3.55	±	0.18		3.62	±	0.25	3.62	±	0.16		3.84	±	0.15	[b]	**
PNW11																
No. of offspring examined	10				10			10				10				
T3 (ng/ml)	0.96	±	0.06		0.93	±	0.07	0.88	±	0.05	**	0.89	±	0.06	**	
T4 (ug/dl)	4.77	±	0.70		4.84	±	0.59	5.21	±	0.65		5.20	±	0.98		
TSH (ng/ml)	4.74	±	0.62		5.81	±	1.72	5.36	±	1.11		4.96	±	0.80		
A/G ratio	1.86	±	0.24		1.89	±	0.29	1.74	±	0.16		1.70	±	0.14		
albumin (g/dl)	3.53	±	0.32		3.63	±	0.29	3.82	±	0.34		4.00	±	0.39	**	

[a] Mean ± SD.
[b] n=9
Abbreviations: HBCD, hexabromocyclododecane; PNW, postnatal week.
*,** Significantly different from the controls by Dunnett's test or Dunnett-type rank-sum test (*p<0.05, **p<0.01).

Table 6　Histopathology of the thymus and spleen of male and female rats perinatally exposed to hexabromocyclododecane (HBCD)

	HBCD in diet (ppm)			
	0	100	1000	10000
HBCD 3				
No. of animals examined (male/female)	10/10	10/10	10/10	10/10
Thymus				
Increased starry sky appearance (±)[a]	0/0[b]	0/0	4*/0	1/0
Spleen				
Atrophy of white pulp (±)	0/0	0/0	0/0	1/0
Reduction in the number of white pulp (±)	0/0	0/0	0/0	1/0
HBCD 11				
No. of animals examined (male/female)	10/10	10/10	10/10	10/10
Thymus				
Increased starry sky appearance (±)	0/0	0/0	0/3	0/0
Reduction of cortical area (±)	1/2	0/0	1/1	4/3
Spleen				
No abnormalities detected	10/10	10/10	10/10	10/10

[a] Grade of change; ±, minimal.
[b] Total No. of animals with each finding.
* Significantly different from the controls by Fisher's exact probability test (*p < 0.05).

ラットの免疫系への影響を，リンパ球のポピュレーション，サブポピュレーション，NK細胞の割合の解析により検討した．その結果，胸腺，脾臓重量に対照群との間に差は認められなかったが，３週令の脾臓においてNK細胞の減少が観察され，末梢血の活性化Ｔ細胞の減少，非活性化Ｂ細胞の上昇も観察された．甲状腺機能障害性を有する薬物Propylthiouracil（PTU）及びMethimazole（MMI）[8,9]を用いた同様の実験では，Ｂ細胞の比率の低下等の大きなポピュレーション変化を伴う現象が観察されたが，それら抗甲状腺作用薬に比較してHBCDの影響は軽度であった．回復期の11週令においては，リンパ球ポピュレーションに有意な変化は観察されなかった．以上，HBCDは，軽度ではあるが，免疫担当細胞への影響が示唆されるデータが得られ，甲状腺ホルモンT3の低下と連動することから，これら影響は，甲状腺機能抑制と連関する可能性が考えられた．なお，血清アルブミンの上昇，肝臓の臓器重量の増加も観察されたことから，HBCDの甲状腺機能への影響は，HBCDが直接甲状腺機能を抑制している可能性と，肝重量が増加していたことから，肝臓の薬物代謝酵素誘導により甲状腺ホルモンが代謝されて血中濃度が減少する二次的影響の可能性の２つが考えられた．

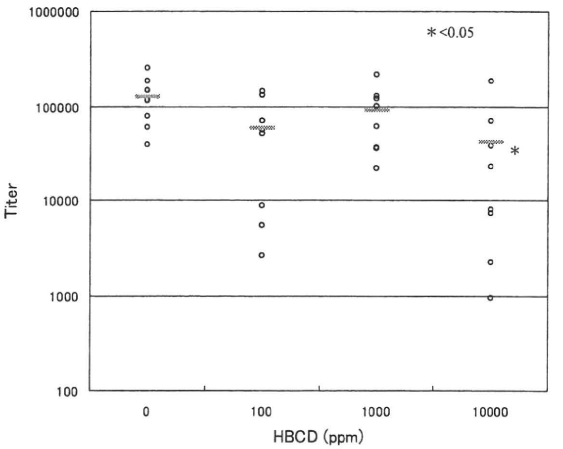

Fig. 2 Effect of HBCD on the antibody production of the offspring
The HBCD-exposed female offspring were challanged with 50μg of KLH with 1 mg of alam twice after ceasing exposure on postnatal day 23 and 33. Serum was obtained 1 week after final immunization, and the IgG titer to KLH was measured by ELISA. Open circles represent individual values, and gray lines indicate mean values. In the highest dose (10000 ppm), the antibody titer against KLH decreased in comparison with the control group significantly (Dunnett, $p<0.05$).

Table 7 Immunity-related influences exposed to HBCD(a) and DBDE (b)

a）HBCD	1000ppm	10000ppm
PNW3		
liver weight	↑	↑
spleen CD161+NK cell		↓
peripheral active T cell		↓
peripheral inactive B cell		↑
serum T3 level		↓
serum TSH level, albumin		↑
serum T3 level	↓	↓
serum albumin		↑
PNW3-7		
KLH-antibody production		↓

b）DBDE	100ppm	1000ppm
PNW3		
liver weight	↑	↑
spleen active T, B cell		↓
spleen CD4+ cell		↓
serum T3 level		↓
PNW11		
peripheral CD161+NK cell		↓
serum T4 level		↓

以上，HBCDは，高濃度暴露において，幼児期ラットに対し免疫抑制影響を示すことが示唆された．また，DBDEも同様の免疫影響を示すが，HBCDの方がDBDEに比べ回復が早い傾向にあることが示された．

HBCDの用量依存性が得られた免疫影響関連の結果をまとめたものを表７a)に示した．また，表７b)には，比較のために同じく用量依存性の免疫影響の得られたDBDEの結果[5]を示した．HBCD，DBDEともに，３週令で甲状腺機能抑制活性と連関すると思われる活性化Ｔ細胞群の低下がみられ，HBCDでは抗体産生の低下がみられた．NK細胞の割合の低下も両化合物でみられたが，HBCDの場合は３週令での抑制が11週令で回復しているのに比べ，DBDEの場合は11週令でも抑制が有意であるという違いがみられた．

謝辞

本研究は厚生労働科学研究費化学物質リスク研究事業の助成を受けて行った．

文献

1）Ema M, Fujii S, Hirata-Koizumi M, Matsumoto M.: Two-generation reproductive toxicity study of the flame retardant hexabromocyclododecane in rats. *Reprod Toxicol.*, 25, 335-351, 2008

2）Birnbaum L.S. et al.: Brominated flame retardants: Cause for concern? *Environ. Health Perspect.*, 112, 9-17, 2004

3）Teshima R., Nakamura R., Nakamura R., Hachisuka A., Sawada J., Shibutani M.: Effects of exposure to decabromodiphenyl ether on the developmental of the immune system in rats. *J. Health Sci.*, 54,

382-389, 2008

4) Ikeda T., Nishikawa A., Imazawa T., Kimura S. and Hirose M.: Dramatic synergism between excess soybean intake and iodine deficiency on the development of rat thyroid hyperplasia. Carcinogenesis, 21, 707-713, 2000

5) Ulrich P. et al.: Validation of immune function testing during a 4-week oral toxicity study with FK506. *Toxicol. Lett.*, 149, 123-131, 2004

6) Dieckmann D. et al.: Activated CD4 CD25 T cells suppress antigen-specific CD4 and CD8 T cells but induce a suppressive phenotype only CD4 T cells. *Immunology*, 15, 305-314, 2005

7) Ohashi H., Itoh M.: Effects of thyroid hormones on the lymphocyte phenotypes in rats: changes in lymphocyte subsets related to thyroid hormone. *Endocrine regulat.*, 28, 117-123, 1994

8) Rooney A.A. et al.: Neonatal exposure to propylthiouracil induces a shift in lymphoid cell subpopulations in the developing postnatal male rat spleen and thymus. Cell. *Immunology*, 223, 91-102, 2003

9) Volpe R.: The immunomodulatory effects of antithyroid drugs are mediated via actions on thyroid cells, affecting thyrocyte-immunocyte signaling: review. *Curr. Pharm.Des.*, 7, 451-460, 2001

International Immunopharmacology 10 (2010) 393–397

Contents lists available at ScienceDirect

International Immunopharmacology

journal homepage: www.elsevier.com/locate/intimp

Effects of tetrabromobisphenol A, a brominated flame retardant, on the immune response to respiratory syncytial virus infection in mice

Wataru Watanabe [a], Tomomi Shimizu [b], Rie Sawamura [b], Akane Hino [b], Katsuhiko Konno [c], Akihiko Hirose [d], Masahiko Kurokawa [b,*]

[a] Department of Microbiology, School of Pharmaceutical Sciences, Kyushu University of Health and Welfare, Yoshino 1714-1, Nobeoka, Miyazaki 882-8508, Japan
[b] Department of Biochemistry, School of Pharmaceutical Sciences, Kyushu University of Health and Welfare, Yoshino 1714-1, Nobeoka, Miyazaki 882-8508, Japan
[c] Department of Clinically Veterinary Medicine, School of Pharmaceutical Sciences, Kyushu University of Health and Welfare, Yoshino 1714-1, Nobeoka, Miyazaki 882-8508, Japan
[d] Division of Risk Assessment, Biological Safety Research Center, National Institute of Health Sciences, 1-18-1, Kamiyoga, Setagaya-ku, Tokyo 158-8501, Japan

ARTICLE INFO

Article history:
Received 1 December 2009
Accepted 28 December 2009

Keywords:
Respiratory syncytial virus
Tetrabromobisphenol A
Pneumonia
Cytokines
Double-positive CD4+CD8+ cells

ABSTRACT

Effects of the brominated flame retardants (BFRs), decabrominated diphenyl ether (DBDE), hexabromocyclododecane (HBCD), and tetrabromobisphenol A (TBBPA), on host immunity of mice were evaluated using respiratory syncytial virus (RSV) infection. Five-week-old female mice were fed a diet containing 1% BFRs for 28 days, and subsequently infected with RSV. No toxicological sign was observed in BFR-treated mice before infection. TBBPA significantly increased the pulmonary viral titer in the infected mice on day 5 post-infection, but DBDE and HBCD did not. Slight histological changes were observed in lung tissues of TBBPA-treated mice with mock infection. These changes due to TBBPA were much exacerbated by RSV infection. Cytokine analysis of bronchoalveolar lavage fluid (BALF) from RSV-infected mice treated with or without TBBPA revealed that TBBPA significantly increased the levels of tumor necrosis factor (TNF)-α, interleukin (IL)-6 and interferon (IFN)-γ at each time point after virus infection, but no change was observed for IL-1β and IL-12. The levels of IL-4 and IL-10, Th2 cytokines, significantly decreased. Thus, TBBPA caused unusual production of the various cytokines in RSV-infected mice. Flow cytometry revealed that the percentage of double-positive CD4+CD8+ cells, immature T lymphocytes, in the cell populations in BALF from RSV-infected mice increased due to TBBPA treatment. The change was not observed in spleen cells of TBBPA-treated mice. The response to RSV infection verified that TBBPA treatment affected the host immunity of mice. Irregular changes in cytokine production and immune cell populations due to TBBPA treatment were suggested to cause exacerbation of pneumonia in RSV-infected mice.

1. Introduction

Human respiratory syncytial virus (RSV), a member of the family *Paramyxoviridae*, is the most prevalent infectious agent of acute lower respiratory illness in infants and young children [1]. Infection and reinfection with RSV are frequent during the first few years of life, and most children are infected by 24 months of age [2]. Clinically severe RSV infection is seen primarily in young children with naïve immune systems and/or genetic predispositions [3], patients with suppressed T-cell immunity [1], and the elderly [4]. A murine model of RSV infection has been used to develop anti-viral drugs and vaccines [5]. In this murine model, the development of pneumonia reflects the severity of RSV infection, and the pneumonia is histopathologically similar to that in humans [6,7]. We previously demonstrated that the severity of the RSV infection significantly reflected the host immune condition [8]. This RSV infection mouse model was shown to be useful to evaluate the immunotoxicity of chemical compounds [9].

Recently, it was reported that long-term exposure to industrial compounds containing brominated flame retardants (BFRs) may be toxic to humans, especially infants and children [10]. There are five major BFRs, tetrabromobisphenol A (TBBPA), hexabromocyclododecane (HBCD), and three commercial mixtures of polybrominated diphenyl ethers (PBDEs), which are known as decabromodiphenyl ether (DBDE), octabromodiphenyl ether (OBDE), and pentabromodiphenyl ether (pentaBDE). They are used as additive or reactive components in a variety of polymers, such as polystyrene foams, high-impact polystyrene, and epoxy resins [10]. BFRs are ubiquitously used as industrial materials worldwide. TBBPA accounted for approximately 76% of the BFRs consumed in Asia in 2001, and the amount used was approximately 90,000 tons [10]. BFRs are easily released into an environment due to deterioration or abrasion of the materials, but there is limited knowledge about their effects on health, particularly their effects on the immune systems of mammals [11–13]. To evaluate human health damage due to this environmental contaminant, the

* Corresponding author. Tel.: +81 982 23 5578; fax: +81 982 23 5684.
E-mail address: b2mk@phoenix.ac.jp (M. Kurokawa).

1567-5769/$ – see front matter © 2010 Elsevier B.V. All rights reserved.
doi:10.1016/j.intimp.2009.12.014

mechanism of action of BFRs on the immune system needs to be clarified.

In this study, the effects of DBDE, HBCD and TBBPA on host immunity were comparatively evaluated using the RSV infection mouse model.

2. Materials and methods

2.1. Mice

Female (4 weeks old) BALB/c mice were purchased from Kyudo Animal Laboratory (Kumamoto, Japan) and housed at 25 ± 2 °C. The mice were allowed free access to a conventional solid diet CRF-1 (Oriental Yeast Co., Chiba, Japan) and water and used in this experiment after 7 days acclimation. The animal experimentation guideline of the Kyushu University of Health and Welfare was followed in the animal studies.

2.2. Cells and virus

Human epidermoid carcinoma (HEp-2) cells (American Type Culture Collection CCL-23) were purchased from Dainippon Pharmaceutical (Osaka, Japan) and maintained in Eagle's minimum essential medium supplemented with heat-inactivated 10% fetal calf serum (FCS). The A2 strain of RSV was obtained from American Type Culture Collection (Rockville, MD) and grown in HEp-2 cell cultures. Viral titers of HEp-2 cells were measured by the plaque method, and expressed as plaque-forming units per milliliter (PFU/ml) [8].

2.3. BFRs

DBDE was purchased from Wako Pure Chemicals (Osaka, Japan). HBCD and TBBPA were purchased from Tokyo Kasei (Tokyo, Japan). They were mixed into a powder diet, which was soy-free to avoid the estrogen-like effect of soybeans, based on the formulation of the NIH-07 open-formula rodent diet [14] and produced by Oriental Yeast Co (Chiba, Japan).

2.4. Animal tests

Five-week-old female mice were fed a soy-free diet mixed with 1% DBDE, HBCD or TBBPA for 4 weeks. After treatment, these mice were fed CRF-1 and used for the following RSV infection test. Throughout the experiments, both chows and drinking water were given ad libitum.

The RSV infection test was performed as reported previously [9]. Briefly, 9-week-old female mice were infected intranasally with 1×10^6 or 1×10^5 PFU per 0.1 ml of the A2 strain of RSV under anesthesia. Mock-infected mice were also inoculated intranasally with 0.1 ml of phosphate-buffered saline (PBS) under anesthesia. On days 1, 3, 5 and 7 after infection, bronchoalveolar lavage fluid (BALF) was obtained from the mice under anesthesia by instilling of 1.0 ml of cold PBS into the lungs and aspirating it from the trachea using a tracheal cannula [15]. Ice-cold BALF was centrifuged at $100\times g$ at 4 °C for 10 min. After centrifugation, the supernatant was stored at −80 °C until to use. The cell pellet was suspended in PBS on ice and used as bronchoalveolar lavage (BAL) cells. For virus titration, the lungs were removed on day 5 post-infection, immediately frozen in liquid N_2, and stored at −80 °C. Frozen lung tissue was homogenized with cold quartz sand in a homogenizer, and viral titers in the supernatants of the homogenates were measured by a plaque assay [8]. The spleen was removed and minced by a scissor to obtain the cell suspension. A single cell suspension of spleen in ice-cold PBS was prepared by the filtration through a sterilized nylon-mesh.

2.5. Histological methods

For histological examination of the infected lungs, mock- or RSV-infected mice were sacrificed on day 5 post-infection, and lungs were removed and placed in buffered formalin for a minimum of 24 h. The tissue was then embedded in low-melting point paraffin, sectioned at a thickness of 5 μm, and stained with hematoxylin and eosin.

2.6. ELISA

Interleukin (IL)-1β, IL-4, IL-6, IL-10, interferon (IFN)-γ and tumor necrosis factor (TNF)-α levels in BALF were measured using specific ELISA kits (Ready-set-go, eBioscience Inc., San Diego, CA) according to the manufacturer's instructions. IL-12 levels in BALF were also measured using a specific kit (Ready-set-go, eBioscience Inc.) for IL-12 p70, without interference by p40 monomer or the related protein IL-23, according to the manufacturer's instructions. These products were tested and found to conform to all eBioscience Inc. quality control release specifications. The lower limits of detection sensitivity in the kits are 8 (pg/mL) for IL-1β, 4 (pg/mL) for IL-4, 4 (pg/mL) for IL-6, 8 (pg/mL) for IL-10, 15 (pg/mL) for IL-12 p70, 4 (pg/mL) for IFN-γ, and 8 (pg/mL) for TNF-α. The intra- and inter-assay coefficients of variation for these ELISA were less than 10%.

2.7. Flow cytometric analysis of BAL and spleen cells

Two-color analysis of BAL cells and spleen cells was performed using a FACS Calibur 3S flow cytometer (Becton Dickinson, Sunnyvale, CA). The following antibodies were used for phenotyping of murine cells: phycoerythrin (PE)-labeled hamster anti-CD3 (145-2C11), rat anti-CD8 (53.6), rat anti-CD11b (M1/70) and rat anti-CD49b (DX5) antibodies, fluorescein isothiocyanate (FITC)-labeled rat anti-CD4 (L3T4) and rat anti-CD25 (7D4) antibodies. All antibodies were purchased from BD Bioscience Pharmingen (San Diego, CA). Samples for analysis were prepared according to the manufacturer's instructions. Briefly, 0.05 ml of a single cell suspension (5×10^5 cells) in PBS was incubated with 0.02 ml of each PE-labeled antibody at 4 °C for 30 min. After incubation, the cells were washed with PBS and then incubated with 0.02 ml of each FITC-labeled antibody at 4 °C for 30 min. The cells were then washed as described above. After staining, at least 10,000 cells suspended in PBS on ice were analyzed by FACS. Finally, the data were analyzed with Cellquest software.

2.8. Statistical analysis

Comparisons of pulmonary viral titers and the levels of cytokines of the control and experimental groups were carried out using Student's *t*-test. A *P* value of 0.05 or less was considered to be significant.

3. Results

3.1. Effects of BFRs on RSV infection in mice

The effects of three BFRs on the severity of RSV infection in mice were investigated. Five-week-old female BALB/c mice were fed a diet containing 1% DBDE, HBCD, or TBBPA for 28 days. No loss of body weight at 28 day or decrease in food consumption during the treatment was detected in BFR-treated mice (Table 1). No particular toxicological sign, such as tremor, or abnormal behavior was observed in these mice either. Then, the mice were intranasally infected with

Table 1
Body weights and food consumption of DBDE-, HBCD- and TBBPA-treated mice.[a]

Index	Experiment 1			Experiment 2	
	Control	DBDE	HBCD	Control	TBBPA
Body weight (g)	20.8 ± 1.1	21.9 ± 1.2	21.2 ± 0.6	20.3 ± 1.1	19.6 ± 0.9
Food consumption (g/week)	25.7 ± 0.3	26.4 ± 0.5	26.8 ± 0.4	24.1 ± 4.1	25.1 ± 2.2

[a] Values represent mean ± standard deviation of 6–7 mice.

the A2 strain of RSV at 1×10^6 PFU. On day 5 after RSV infection, pulmonary viral titers were significantly ($P<0.001$) increased in TBBPA-treated mice compared with the control (Table 2). However, an obvious increase in the pulmonary viral titers was not observed in DBDE- or HBCD-treated mice. To confirm the effects of TBBPA on RSV infection, an additional group was instilled with a low titer (1×10^5 PFU) of RSV (Table 2). The pulmonary viral titers in low-titer TBBPA-treated mice were significantly ($P<0.05$) higher than those in control mice as well. Then, to investigate whether TBBPA directly promotes the growth of virus, the effect of TBBPA on the replication of RSV was tested in vitro using HEp-2 cell cultures, with the result that the compound did not affect the growth of RSV (data not shown). Thus, although BFRs did not show any apparent toxicity in mice in this study, TBBPA increased the RSV titers in the lung tissues of RSV-infected mice.

3.2. Effects of TBBPA on the development of pneumonia in RSV-infected mice

The effects of TBBPA ingestion on lung tissues of RSV-infected mice were analyzed histopathologically. While typical features of pneumonia such as infiltrations of lymphocytes and neutrophils due to RSV infection were observed on day 5 post-infection in mice treated with and without TBBPA (Fig. 1a, b), severely exacerbated pneumonia with expansion of the inflammation and hyperplasia of macrophages were found in the infected mice treated with TBBPA (Fig. 1b). In mock-infected mice, mild inflammation and congestion were observed in TBBPA-treated mice compared with the control (Fig. 1c, d). These results indicated that TBBPA caused mild immune injury in lung tissues and that the lesion was exacerbated to severe pneumonia by RSV infection in mice.

3.3. Effects of TBBPA on levels of cytokines in BALF from RSV-infected mice

To investigate the effects of TBBPA on the immune system, the levels of various cytokines in BALF induced by RSV infection in mice treated with TBBPA were measured by ELISA on day 1, 3, 5 and 7 post-infection (Table 3). The levels of IFN-γ, a representative marker of pneumonia due to RSV infection, in BALF from TBBPA-treated mice were significantly ($P<0.01$) increased and approximately 5.2-fold of the control on day 5 post-infection. IFN-γ could not be detected in BALF from mock-infected mice with or without TBBPA treatment (data not shown). On day 1 post-infection, the levels of both TNF-α and IL-6 in TBBPA-treated mice were significantly ($P<0.05$) increased to 5.8- and 2.6 times, respectively, of the control. No significant increase of IL-1β or IL-12 was found after TBBPA treatment. In contrast to these results, the levels of both IL-4 and IL-10, Th2 cytokines, were significantly ($P<0.05$) reduced on day 7 post-infection in BALF from TBBPA-treated mice compared with the control. Thus, TBBPA treatment enhanced production of TNF-α, IL-6 and IFN-γ but suppressed production of IL-4 and IL-10 in RSV-infected mice.

Table 2
Effects of treatment of DBDE, HBCD and TBBPA on pulmonary viral titers on day 5 post-infection in RSV-infected mice.[a]

Group/BFRs treatment	Pulmonary viral titers (PFU/ml)		
	Experiment 1	Experiment 2	Experiment 3
Control	14,833 ± 8,566	17,433 ± 3,670	526 ± 146
DBDE	19,111 ± 18,000	ND	ND
HBCD	13,875 ± 2,776	ND	ND
TBBPA	ND	34,967 ± 7742**	1630 ± 764*

*Statistically different from control at $P<0.05$ (Student's t-test).
**Statistically different from control at $P<0.001$ (Student's t-test).
[a] Values represent mean ± standard deviation of 6–7 mice. Mice were infected intranasally with 1×10^6 PFU of RSV in experiments 1 and 2, and with 1×10^5 PFU in experiment 3. ND, not determined.

3.4. Effect of TBBPA on cell populations in BAL and spleen cells in RSV-infected mice

To clarify the effects of TBBPA on immune responses in RSV-infected mice, the cell populations of BAL and spleen cells were analyzed on days 1 and 3 post-infection by flow cytometry (Table 4). There were no significant differences in the number of BAL cells in control and TBBPA-treated mice groups in RSV-infected mice (data not shown). On day 1 post-infection, CD11b+ (positive) cells, dendritic cells or macrophages, accounted for more than 90% of BAL cells, and a difference in the population ratios of the control and TBBPA-treated mice was not observed. However, the percentages of double-positive T cells (CD4+CD8+), immature T cells, were markedly increased in BAL cells from RSV-infected mice due to treatment with TBBPA on day 3 post-infection, although there was no difference the number of CD4+CD8+ cells in mock-infected mice. The percentages of CD49b+ cells, NK cells, in BAL cells on days 1 and 3 post-infection were not affected by treatment with TBBPA. Although TBBPA reduced the ratio of CD3+CD25+ cells, activated T cells, on day 1 post-infection, they were low overall in BALF from RSV-infected mice. To evaluate the effects of TBBPA treatment on systemic immunity, CD11b+ and CD4+CD8+ cells in spleens of mock- and RSV-infected mice were analyzed on day 3 post-infection, but no difference due to TBBPA treatment was observed in the treated mice.

4. Discussion

To evaluate the effects of three BFRs on the host immunity of mice, a murine RSV infection model was used in this study [8,9]. Although mice were fed a diet containing 1% BFR for 4 weeks, no toxicity was observed in the BFR-treated mice (Table 1). The dosage of BFRs based on the average food consumption and body weight was calculated at approximately 1700 mg/kg/day (Table 1). The dosage sounds very high, but these BFRs were reported to be non-toxic in mice at this dosage for this treatment period [16,17], and our results were consistent with the reports. However, a significant ($P<0.001$) increase of pulmonary viral titers was detected in TBBPA-treated mice compared with the control, but not in DBDE- or HBCD-treated mice (Table 2). Consequently, it was verified that TBBPA treatment enhanced RSV growth in the lungs of mice.

In a histopathological analysis, mild lesions of the lungs were detected after TBBPA treatment in mock-infected mice (Fig. 1). Moreover, the administration of TBBPA was shown clearly to increase virus titers in the lungs (Table 2) and exacerbate the pneumonia in RSV-infected mice. Previously, treatment with an immunosuppressive agent, cyclophosphamide, was shown to increase pulmonary viral titers and exacerbate the pneumonia in RSV-infected mice [5,8]. This suggests that immune conditions in the host contribute to pulmonary virus titers and exacerbation of pneumonia. Thus, TBBPA might induce a disorder of the immunity against RSV infection, resulting in the increase of virus titers and exacerbation of pneumonia.

To clarify the immune disorder due to TBBPA administration, cytokine productions induced by RSV infection were examined (Table 3). In TBBPA-treated mice, marked increases of IL-6 and TNF-α were observed on day 1 post-infection. It was reported that these cytokines increase immediately in the early phase after RSV infection [18,19]. On the other hand, productions of IL-1β and IL-12, which are produced mainly by macrophages and dendritic cells, were not affected by TBBPA. As reported previously [8,9], the levels of IFN-γ, a marker of pneumonia, increased maximally on day 5 post-infection in RSV-infected mice, and its production was enhanced in TBBPA-treated mice (Table 3). The increase of IFN-γ may be induced by the increased IL-6 and TNF-α. Thus, these irregular cytokine productions indicate